Catal Lett (2011) 141:1442–1450
DOI 10.1007/s10562-011-0676-1

Epoxidation of Butadiene with Hydrogen Peroxide Catalyzed by the Salts of Phosphotungstate Anions: Relation Between Catalytic Activity and Composition of Intermediate Peroxo Complexes

Lidia I. Kuznetsova · Nina I. Kuznetsova ·
Raisa I. Maksimovskaya · Galina I. Aleshina ·
Olga S. Koscheeva · Viktor A. Utkin

Received: 14 June 2011 / Accepted: 22 July 2011 / Published online: 11 August 2011

Abstract Epoxidation of 1,3-butadiene has been studied in acetonitrile solutions of aqueous H_2O_2 and tetrabutylammonium or 1-ethyl-3-methylimidazolium salts of phosphotungstate anions: $[(n\text{-}C_4H_9)_4N]_3\{PO_4[WO(O_2)_2]_4\}$, $[(n\text{-}C_4H_9)_4N]_5Na_{0.6}H_{1.4}[PW_{11}O_{39}]$ or $[(C_2H_5)(CH_3)C_3H_3N_2]_5NaH[PW_{11}O_{39}]$. The selectivity of the 1,3-butadiene to 3,4-epoxy-1-butene (EpB) conversion attains 97% at nearly 100% efficiency of the H_2O_2 consumption. The rate of the EpB formation has been correlated with the solution compositions as found by ^{31}P NMR under the reaction conditions.

Keywords Epoxidation · 1,3-Butadiene · Hydrogen peroxide · Phosphotungstates · Tetrabutylammonium · 1-Ethyl-3-methylimidazolium · ^{31}P NMR

1 Introduction

Oxidation of 1,3-butadiene (BD) to 3,4-epoxy-1-butene (EpB) opens a path to valuable C_4-oxygenates such as 3-butene-1,2-diol and 2-butene-1,4-diol [1–3] and 2,5-dihydrofuran [4]. Gas-phase epoxidation of BD has been realized on silver catalysts [5, 6]. At the same time, it is reasonable to consider a liquid-phase oxidation of BD to EpB because of a newly developed low-cost manufacturing of H_2O_2 from O_2 and H_2 gases and the appropriate interest to studies of epoxidation of terminal and cyclic olefins [6–16]. Specific problem of BD is its strong reactivity with respect to side transformations. Catalysts and radical intermediates can initiate non-selective oxidation with a breakup of the hydrocarbon chain [17]. Resulting loss of selectivity may limit application of liquid-phase systems to obtaining EpB. To our knowledge, there are only two examples of liquid-phase epoxidation of BD. EpB forms as a main product of the BD oxidation with H_2O_2 over titanium silicate TS-1 in CH_3OH [7] and in CH_3CN solution of $[TBA]_4[\gamma\text{-}SiW_{10}O_{34}(H_2O)_2]$ [11]. No detailed information is available concerning the BD epoxidation in the presence of polyoxometalates.

The aim of our work was to determine the main variables affecting the BD epoxidation with hydrogen peroxide. Phosphotungstates were used as catalysts because of their ability to combine strongly electrophilic character of active peroxide intermediates with low catalytic activity in radical decomposition of H_2O_2 [18–25]. We also followed carefully the side reactions of BD conversion and H_2O_2 decomposition.

Catalytic action of phosphotungstates in epoxidation of olefins with H_2O_2 is usually associated with peroxo anion $\{PO_4[WO(O_2)_2]_4\}^{3-}$ that was firstly isolated and characterized by Venturello and coworkers [20]. Formation of other peroxo phosphotungstate anions $[PW_nO_m]^{x-}$ ($n < 4$) in H_2O_2 solutions is well known [22, 23, 26–28], but their role in catalysis is not clear [24, 28, 29]. It was shown [27] that stoichiometric epoxidation of 1-octene by $\{PO_4[WO(O_2)_2]_4\}^{3-}$ resulted in degradation of the complex to poorly active mixture of PW_n species. The suggestion has

---

Electronic supplementary material The online version of this article (doi:10.1007/s10562-011-0676-1) contains supplementary material, which is available to authorized users.

L. I. Kuznetsova (✉) · N. I. Kuznetsova ·
R. I. Maksimovskaya · G. I. Aleshina · V. A. Utkin
Boreskov Institute of Catalysis SB RAS, Acad. Lavrentiev Prosp., 5, Novosibirsk 630090, Russia
e-mail: livkuzn@catalysis.nsk.su

O. S. Koscheeva
Nikolaev Institute of Inorganic Chemistry SB RAS, Acad. Lavrentiev Prosp., 3, Novosibirsk 630090, Russia

been made [27] that the active $\{PO_4[WO(O_2)_2]_4\}^{3-}$complex is rapidly regenerated with H_2O_2 under the phase transfer catalytic conditions. In this connection, the second aim of our work was a direct observation by ^{31}P NMR of transformations of the phosphotungstate anions in the process of the catalytic BD epoxidation.

We studied epoxidation of BD with aqueous hydrogen peroxide in CH_3CN solutions using well characterized tetrabutylammonium (TBA^+) and 1-ethyl-3-methylimidazolium ($EMIm^+$) salts of phosphotungstate anions: $[(n\text{-}C_4H_9)_4N]_3\{PO_4[WO(O_2)_2]_4\}$, $[(n\text{-}C_4H_9)_4N]_5Na_{0.6}H_{1.4}[PW_{11}O_{39}]$, and $[(C_2H_5)(CH_3)C_3H_3N]_5NaH[PW_{11}O_{39}]$. The rate of the BD epoxidation has been analyzed in connection with the composition of active peroxo complex intermediates. To determine the effect of a cationic moiety on the catalytic performance, we tested TBA^+ and $EMIm^+$ salts of $[PW_{11}O_{39}]^{7-}$ anion. The motivation for this study was positive effect of imidazolium salts (ionic liquids) used as solvents in a number of peroxide reactions [13, 30–35].

2 Experimental

2.1 Materials and Reagents

Commercial chemically pure $H_3[PW_{12}O_{40}]\cdot nH_2O$ and H_3PO_4, $(n\text{-}C_4H_9)_4NBr$ of a reagent grade, unstabilized ~34% aqueous H_2O_2 of special purity (Reachim), CH_3CN of high purity (Kriochrom) and 1,3-butadiene (Aldrich) were used. $Na_7[PW_{11}O_{39}]$ (Na-PW_{11}) was prepared as usual, by mixing $H_3[PW_{12}O_{40}]$ and H_3PO_4 aqueous solutions in atomic ratio P/W = 1/11 and adding Na_2CO_3 to pH 4, with subsequent heating at 90 °C for 1 h. ^{31}P NMR: a single peak −10.9 ppm [36] (Fig. S1, a).

The $[(n\text{-}C_4H_9)_4N](NO_3)$ solution was prepared from the $[(n\text{-}C_4H_9)_4N]Br$ solution by adding equimolar amount of $AgNO_3$ in solution and separating the AgBr residue.

EMImBr was prepared in the same way as described in [37] for BMImCl. ^{1}H NMR, [$^2H_6$] Dimethylsulfoxide, as in [38] δ: 9.27 ($NC\underline{H}N$), 7.84 ($CH_3NC\underline{H}CHN$), 7.75 ($CH_3NCHC\underline{H}N$), 4.22 ($NC\underline{H}_2CH_3$), 3.88 ($NC\underline{H}_3$), 1.42 ($NCH_2C\underline{H}_3$).

2.2 Synthesis of Phosphotungstates

$[(n\text{-}C_4H_9)_4N]_3\{PO_4[WO(O_2)_2]_4\}$ (TBA-PW_4) was prepared via a procedure of Brégeault et al. [22]. Water solution of $H_3[PW_{12}O_{40}]$ (PW_{12}) (6 mmol of W) was mixed with 30% H_2O_2 (100 mmol), and the peroxo complex anion was precipitated with $[(n\text{-}C_4H_9)_4N](NO_3)$ (1.6 mmol). The solid was washed thoroughly with water and dried in air. $C_{48}H_{108}N_3O_{24}PW_4$ (1876.4): calcd. C 30.7, H 5.75, N 2.24, P 1.65, W 39.2; found C 31.4, H 5.90, N 2.24, P 1.64, W 38.7. The IR spectrum (in KBr) agrees with that described previously [22].

$[(n\text{-}C_4H_9)_4N]_2\{HPO_4[WO(O_2)_2]_2\}$ (TBA-PW_2) was prepared as previously described [23]. Water solution of $H_3[PW_{12}O_{40}]$ (0.5 mmol) and H_3PO_4 (30 mmol) was mixed with 30% H_2O_2 (59 mmol), and the peroxo complex anion was precipitated with $[(n\text{-}C_4H_9)_4N](NO_3)$ (10 mmol). The solid was thoroughly washed with water and dried in air. $C_{32}H_{73}N_2O_{14}PW_2$ (1107.7): calcd. C 34.7, H 6.59, N 2.53, P 2.80, W 33.2; found C 34.4, H 6.50, N 2.60, P 2.55, W 33.2. IR spectrum (in Nujol): ν(O–O) bands 842, 851 and 883 cm^{-1} as in [23].

$[(n\text{-}C_4H_9)_4N]_5Na_{0.6}H_{1.4}[PW_{11}O_{39}]$ (TBA-PW_{11}) was prepared by mixing aqueous solutions of $Na_7[PW_{11}O_{39}]$ (pH 4.0, 2.5 mL, 5.8×10^{-4} mol) and $[(n\text{-}C_4H_9)_4N]Br$ in a molar ratio 1:10. The solid formed was washed with water till negative reaction on Br^- ions and dried in air. $C_{80}H_{181.4}N_5Na_{0.6}O_{39}PW_{11}$ (3902.9): calcd. C 24.6, H 4.65, N 1.79, Na 0.353, P 0.794, W 51.8; found: C 24.2, H 4.55, N 1.70, Na 0.320, P 0.674, W 50.8. IR spectrum (in KBr) conformed to the structure of heteropolyanion $[PW_{11}O_{39}]^{7-}$ [39]: ν = 1079 and 1053 (P–O), 957 (W=O), 891, 817 and 754 (W–O–W), 597 δ(O–P–O), 518 δ(W–O–W). ^{31}P NMR: two broad peaks (−12.3 and −12.8 ppm) in dry CH_3CN and a narrow peak (−12.5 ppm) in CH_3CN with water admixture (Fig. S1, b, c).

$[(C_2H_5)(CH_3)C_3H_3N_2]_5NaH[PW_{11}O_{39}]$ (EMIm-PW_{11}) was prepared by mixing aqueous solutions of $Na_7[PW_{11}O_{39}]$ (pH 4.0, 2.5 mL, 5.8×10^{-4} mol) and EMImBr (0.6 mL, 2.9×10^{-3} mol). The precipitated solid was washed with water till negative reaction on Br^- ions and dried in air. $C_{30}H_{56}N_{10}Na_1O_{39}PW_{11}$ (3256.3): calcd. C 11.1, H 1.72, N 4.30, Na 0.71, P 0.952, W 62.1; found C 11.1, H 2.10, N 4.30, Na 0.94, P 0.891, W 57.7. IR (KBr): ν = 1078 and 1037 (P–O), 944 (W=O), 892, 850, 801, 754sh, and 728 (W–O–W), 592 δ(O–P–O), 508 δ(W–O–W) cm^{-1}.

2.3 Catalytic Experiments

Oxidation of BD was carried out in a 28 mL Pyrex reactor equipped with a magnetic stirrer and Teflon valves for connecting to a gas burette and for sampling. Catalysts were dissolved in a mixture of ~34% H_2O_2 (0.1–0.3 mL, 1–3 mmol of H_2O_2) and CH_3CN (2 mL) at the reaction temperature (20–60 °C) for 10 min. The reactor was purged with BD at ambient pressure, the gas burette was filled with BD (measurements in the atmosphere of BD) or argon (measurements at a dosed BD amount of 26 mL, 1 mmol), the system was sealed and the stirrer was on. To minimize diffusion of BD, the valve between the reactor and burette was opened only for several seconds just to fix the BD uptake. The initial rapid gas consumption corresponded to solubility of BD in the reaction mixture

(~0.12 M at 50 °C), the further slower consumption indicated the oxidation of BD. In the course of the reaction, the reaction solution was sampled for GC analysis. The reaction was stopped after 2–5 h.

2.4 Analyses

GC analysis of the reaction solutions was made on a Kristall—2000M instrument equipped with a flame ionization detector and a 0.53 mm × 30 m SPB™—1000 capillary column in the temperature programmed regime. The product amounts were calculated using calibration curves plotted for EpB, furan, acrolein, 3-butene-1,2-diol and 2-butene-1,4-diol. The products were identified by the retention times (by comparison with reference compounds) and by means of GC–MS, using a Chrompack capillary column CP-Sil 24 CB.

Concentration of hydrogen peroxide in the reaction solutions was determined iodometrically. The reaction solution, 0.1 mL, was added to 5 mL of acetic acid containing 0.5 g of KJ and left for 10 min. The mixture with added 50 mL of water was titrated with 0.04 N thiosulfate solution.

2.5 ^{31}P NMR Measurements

The ^{31}P NMR spectra were measured on an Avance-400 Bruker NMR spectrometer at 161.98 MHz, with a 5 kHz sweep width, 10 μs pulse width and 30 s pulse delay. The measurements were done with standard 10 mm o.d. (2.5 mL solution volume) sample tubes. Chemical shifts (δ) were determined relative to 85% H_3PO_4 as an external reference; δ for PW_{12} in CH_3CN with small content of water was equal to -14.65 ppm under our conditions. Admixture of PW_{12} in the analyzed solutions served as additional, internal, reference.

The phosphotungstates were dissolved at 50 °C in CH_3CN containing aqueous H_2O_2 and kept at room temperature or 50 °C for 10 min before recording the spectra.

3 Results and Discussion

Oxidation of BD with H_2O_2 in acetonitrile solution of TBA-PW_4, TBA-PW_{11}, and EMIm-PW_{11} produced mainly EpB (Table 1). The side products were acrolein (1), furan (2), 3-butene-1,2-diol (3) and 2-butene-1,4-oxygenates (4) including 2-butene-1,4-diol, 4-hydroxy-2-butenal and butenedial. 1,3-Butadiene diepoxide and other products of EpB oxidative conversions were not detected. The selectivity of EpB formation was over 80% for TBA-PW_4 (entry 1) and around 90% for TBA-PW_{11} (entry 2) at 20 °C. The amount of EpB grew without loss of the selectivity with elevation of temperature to 60 °C. Substantial amounts of EpB were produced, and conversion of H_2O_2 reached 63 and 84%, with the selectivity of the BD to EpB conversion being still as high as 88 and 91% in entries 3 and 4. Further oxidations were carried out at 50 °C.

Accumulation of the products with time is shown in Fig. 1 for three different catalysts. In the presence of TBA-PW_4, EpB was rapidly accumulated during the initial period, then the process slowed down and came to a stationary mode after 2 h (Fig. 1a). The decrease in the initial catalytic activity was less evident for TBA-PW_{11} and EMIm-PW_{11} (Fig. 1b, c). The estimated from these curves catalytic activity of EMIm-PW_{11} in the production of EpB was about two times higher than that of TBA-PW_{11}.

The side products, acrolein, furan, 3-butene-1,2-diol and 2-butene-1,4-diol, were accumulated as shown in Fig. 1. It could be expected that the side products, particularly diols, appeared from secondary transformations of EpB. However, it was experimentally found that without BD these

Table 1 Products of the BD oxidation in the presence of phosphotungstates

Entry	Catalyst (μmol)	Time (min)	Products (mmo1) × 10^2					S_{BD}	Conv. H_2O_2 (%)	$S_{H_2O_2}$	TON
			EpB	(1)	(2)	(3)	(4)				
1	TBA-PW_4(5.3)	300	5.9	0.6	0.10	0.4	0.06	83	–	–	10
2	TBA-PW_{11}(5.1)	255	2.2	0.2	0.05	0	0	90	–	–	4
3	TBA-PW_{11}(10)	330	51.2	6.0	0.05	0.4	0.3	88	63	88	51
4	EMIm-PW_{11}(10)	300	64.5	6.2	0.2	0	0.2	91	84	90	64

The reaction conditions: 1, 2—~34% aq. H_2O_2 (0.2 mL, 2.12 mmol), 3—~34% aq. H_2O_2 (0.1 mL, 0.92 mmol), 4—~34% aq. H_2O_2 (0.1 mL, 0.86 mmol); CH_3CN (2 mL), 20 °C (1 and 2), 60 °C (3 and 4); under the BD atmosphere

(1) acrolein, (2) furan, (3) 3-butene-1,2-diol, (4) 2-butene-1,4-oxygenates

S_{BD}—EpB formed/total GC detected products, (mol/mol) × 100%

$S_{H_2O_2}$—EpB formed/H_2O_2 consumed (mol/mol) × 100%

TON—Turnover number calculated from epoxide yield

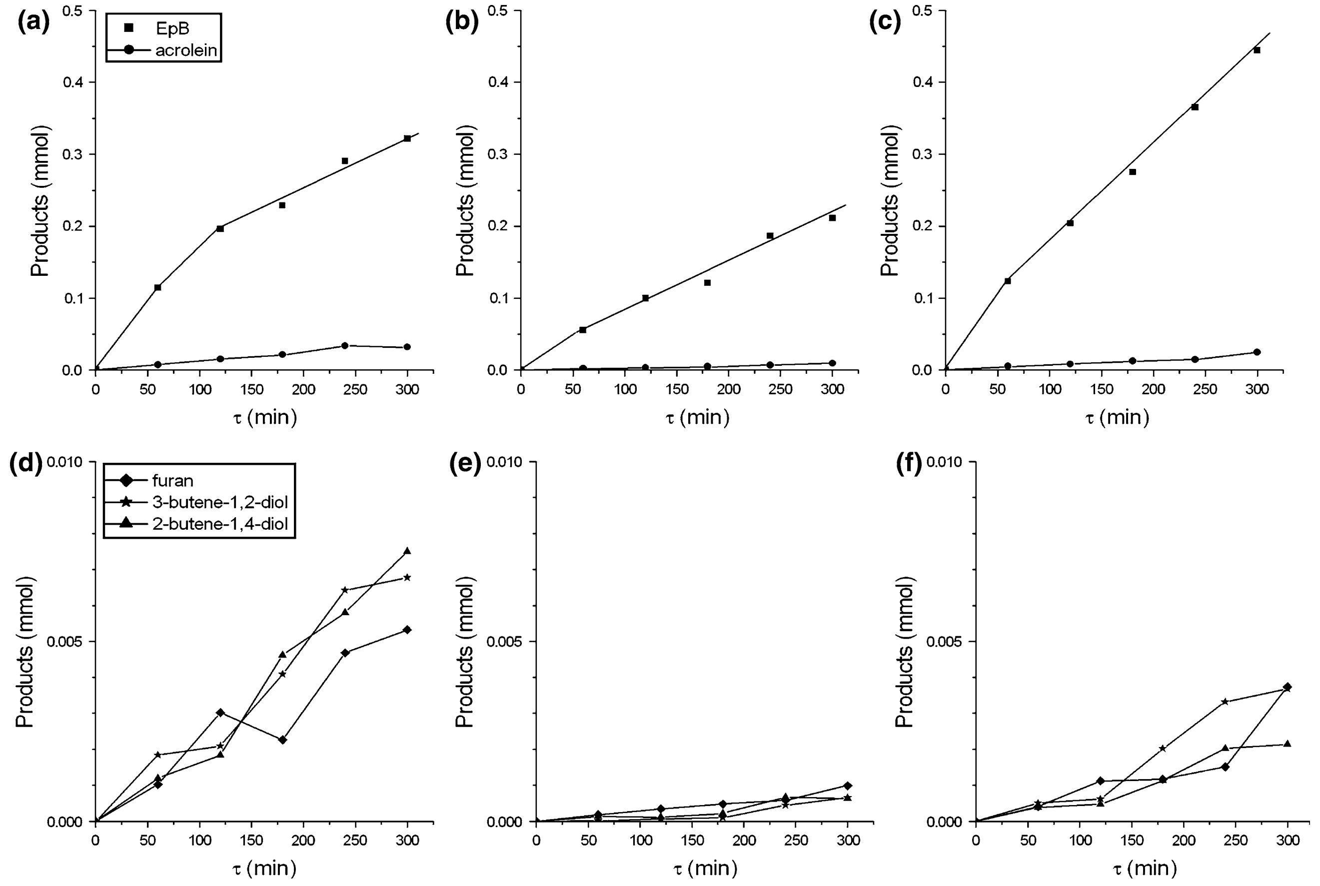

Fig. 1 Time dependence of amounts of 3,4-epoxy-1-butene and acrolein (**a**–**c**), furan, 3-butene-1,2-diol and 2-butene1,4-diol (**d**–**f**) formed at the oxidation of 1,3-butadiene with hydrogen peroxide. Reaction conditions: **a**, **d**—TBA-PW_4 (10 mg, 5.3 μmol), **b**, **e** TBA-PW_{11} (20 mg, 5.1 μmol), **c**, **f** EMIm-PW_{11} (17 mg, 5.0 μmol); CH_3CN (2 mL), ~34% aq. H_2O_2, (0.2 mL, 2 mmol), BD (26 mL, 1 mmol), 50 °C

products were not formed from EpB under the reaction conditions. The side products are supposed to result from a radical pass of the BD oxidation [17, 40]. However the amount of acrolein was 10–30 times lower (Fig. 1a–c) and the total amount of 3-butene-1,2-diol, 2-butene-1,4-diol and furan was 50–200 times lower (Fig. 1d–f) than that of EpB. Only traces of EpB and acrolein (ca. 0.2×10^{-5} mol of each) were obtained under the same conditions in the absence of the catalyst.

The balance account of the EpB production and the main regularities of epoxidation in the presence of the phosphotungstate catalysts are given in Table 2. An important problem in oxidation with H_2O_2 is its unproductive decomposition that is accompanied by evolution of oxygen under the reaction conditions. Under our conditions (0.2 mL ~34% H_2O_2, 2 mL CH_3CN, 50 °C, 2 h), the amount of hydrogen peroxide consumed did not exceed 1% of starting H_2O_2 without catalyst and 10% in the presence of TBA-PW_4, TBA-PW_{11} or EMIm-PW_{11}. It is known that readily oxidized substances serve as traps of radical intermediates, thus inhibiting the chain decomposition of hydrogen peroxide [41, 42]. As expected, the introduction of BD did inhibit decomposition of H_2O_2 in phosphotungstate solutions and reduced the unproductive loss of hydrogen peroxide during the oxidation. Data of Table 2 show that the molar amounts of H_2O_2 consumed and the oxidation products formed are in most cases close to each other, which indicates high efficiency of hydrogen peroxide utilization. Furthermore, the molar amounts of gaseous BD consumed and total amounts of the GC detected products are in close agreement within the accuracy of our measurements. It confirms the absence of high-boiling and hardly detectable by GC products of the BD oligomerization.

Based on the data of Table 2, one can notice a general tendency in variation of characteristics of the oxidation performance with the phosphotungstate composition and loadings of the catalyst and hydrogen peroxide. The total amount of the products strongly depends on the catalyst weight (entries 5, 1 and 6), but weakly depends on starting H_2O_2 concentration (entries 8, 1, 7, and 4, 10), which indicates the almost complete saturation of the catalytically active peroxo complexes with the reactive peroxide groups.

Table 2 The results of the BD epoxidation obtained under variation of the phosphotungstate composition, loading of the catalyst and hydrogen peroxide

Entry	Catalyst (μmol)	H_2O_2 starting (mmol)	H_2O_2 consumed (mmol)	BD consumed (mmol)	GC detected products (mmol)	S_{BD} (%)	$S_{H_2O_2}$ (%)
1	TBA-PW_4, (5.3)	1.91	0.25	0.23	0.21	93	78
2	TBA-PW_{11}, (5.1)	1.91	0.12	0.09	0.09	93	67
3	EMIm-PW_{11} (5.0)	1.94	0.28	0.19	0.22	96	75
4[a]	EMIm-PW_{11} (2.3)	1.98	0.22	0.18	0.16	94	70
5	TBA-PW_4 (2.6)	1.93	0.16	0.10	0.10	86	60
6	TBA-PW_4 (11)	1.99	0.46	0.24	0.33	89	63
7	TBA-PW_4 (5.3)	2.79	0.22	0.13	0.18	87	71
8	TBA-PW_4 (5.3)	1.01	0.13	0.14	0.15	90	~90
9	TBA-PW_{11} (5.1)	0.96	0.09	0.08	0.08	96	78
10[a]	EMIm-PW_{11} (2.3)	1.03	0.16	0.14	0.19	97	~100

The reaction conditions: cat., ~34% aqueous H_2O_2, BD (26 mL, 1 mmol), CH_3CN (2 mL), 50 °C; 2 h or [a] 5 h

S_{BD}—EpB formed/Total GC detected products, (mol/mol) × 100%

$S_{H_2O_2}$—EpB formed/H_2O_2 consumed, (mol/mol) × 100%

The selectivity of the BD to EpB conversion (S_{BD}) is over 90 mol% for all three catalysts at a favorable proportion of hydrogen peroxide and catalyst loading in entries 1–3. Decreasing the catalyst (entry 5) or increasing the H_2O_2 (entry 7) loadings equally lead to growing contribution of radical oxidation of BD and, as a result, to a noticeable loss of the selectivity of the BD to EpB conversion.

The selectivity of the H_2O_2 to EPB formation ($S_{H_2O_2}$) under excess H_2O_2 in entries 1–7, is 63–78 mol%. Negative action of the excess hydrogen peroxide and water introduced together with H_2O_2 on the selectivity of H_2O_2 consumption in the presence of the catalyst is related with radical routes: H_2O_2 decomposition and the BD and solvent oxidation. Taking into account the overall H_2O_2 conversion in Table 2 (entries 1–7), the inefficient consumption of H_2O_2 was on average ~3% from the initial H_2O_2 amount.

The decrease in the starting H_2O_2 concentration increases the selectivity of its consumption to 78% for TBA-PW_{11}, 90% for TBA-PW_4, and ~100% for BMIm-PW_{11} (entries 1 and 8, 2 and 9, 4 and 10). The latter values exceed the appropriate characteristics of catalyst TS-1 [7] and approach the reported selectivity of H_2O_2 utilization in the presence of $[TBA]_4[\gamma\text{-}SiW_{10}O_{34}(H_2O)_2]$, under the H_2O_2 deficient conditions [11].

The phosphotungstate catalysts appeared efficient in CH_3CN solutions, while poor performance was observed in other organic solvents under conditions indicated in Table 1. Reaction of BD with H_2O_2 in *N,N*-dimethylacetamide solution of TBA-PW_4 gave trace amounts of acrolein, furan and EpB. Methanol has been reported to be the perfect medium for catalysis by TS-1 [7], while in methanol solution of TBA-PW_4 no products were obtained under our conditions, except for small amount of products

Table 3 The composition of the phosphotungstate peroxo complexes determined from the ^{31}P NMR spectra in Fig. 2, and released tungstate: before the contact with BD (1–3), under the catalytic reaction (4–6); and the rate of the EpB formation calculated from the curves in Fig. 1: initial, measured for the first hour of the reaction (1–3) and stationary, measured for the further 2–5 h of the reaction (4–6)

Entry	Starting phosphotungstate (2.3 mM)	Content of different complexes (mM)						Rates of EpB formation (mmol L^{-1} h^{-1})
		PW_4	PW_3	PW_2	PW_1	PW_{12}	WO_x	
1	TBA-PW_4	2.3	0	0	0	0	0	52
2	TBA-PW_{11}	0.9	0	0	0	1.4	6.9	24
3	EMIm-PW_{11}	0.9	0.3	0.3	0	0.8	10.5	56
4	TBA-PW_4	0.3	0	1.7	0.3	0	4.3	19
5	TBA-PW_{11}	0	0	0.9	0	1.4	6.7	19
6	EMIm-PW_{11}	0.65	0.65	0.5	0	0.5	13.7	36

arising from the Diels–Alder dimerization of BD. Conversion of H_2O_2 in both latter solvents was $\leq 6\%$.

The state of the phosphotungstate catalysts in the reaction solutions was monitored by the ^{31}P NMR spectroscopy. The concentration of phosphotungstate anions, formed during the reaction with H_2O_2 and BD, was estimated from relative intensities of the ^{31}P NMR peaks assuming that the total spectrum intensity corresponds to molar concentration of the starting phosphotungstate (Table 3). The average error of these measurements was estimated as $\approx \pm 10\%$.

Peroxo complex TBA-PW_4 dissolved in CH_3CN (10 mM) gives a ^{31}P NMR peak at $\delta \approx 3.8$ ppm with two satellites arising from the indirect spin–spin coupling with magnetic tungsten isotope ^{183}W, $^2J_{P\text{–}O\text{–}W} = 18.5$ Hz (Fig. 2, a). The observed satellite to central peak intensity ratio, equal to ~1:3.2:1, corresponds to composition PW_4, in agreement with the published data [22, 26, 27]. After addition of aqueous hydrogen peroxide, the complex remains intact, but its signal shifts to $\delta \approx 3.5$ ppm (Fig. 3a) because of significant dependence of δ on the solvent composition [23, 27]. Additional complexes were detected at ~2 and 0.4 ppm in the presence of H_2O_2 after storing the TBA-PW_4 solution for several days (Fig. 2b). According to relative intensities of the P–O–W coupling satellites, we identified the new species as peroxo

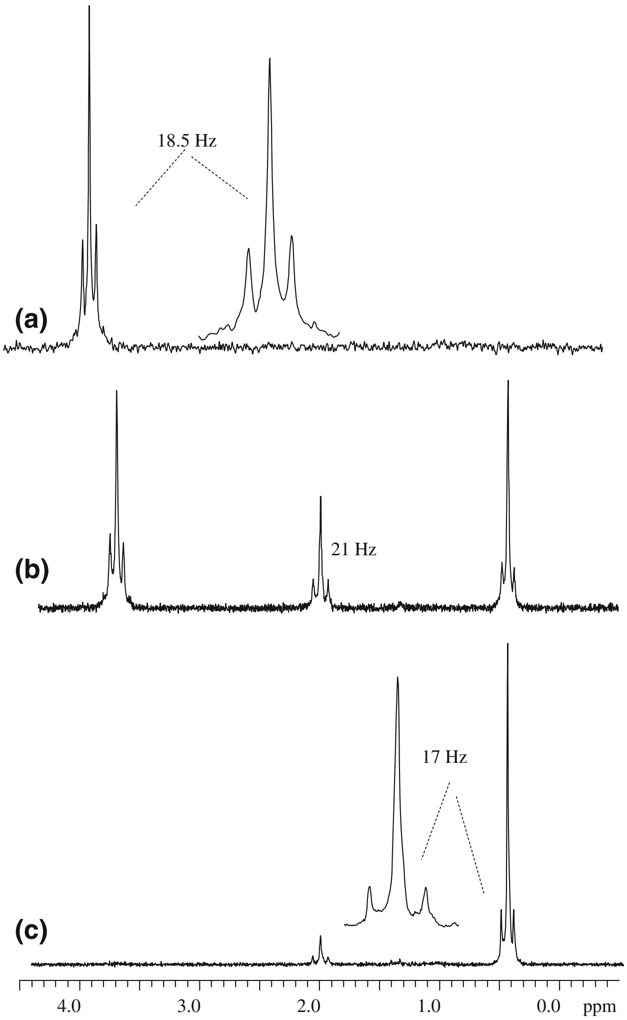

Fig. 2 ^{31}P NMR sygnals of peroxo complexes (10 mM) with $^2J_{P\text{–}O\text{–}W}$ coupling satellites: *a* $[(n\text{-}C_4H_9)_4N]_3\{PO_4[WO(O_2)_2]_4\}$ in CH_3CN, *b* the same complex after storing in $CH_3CN/(\sim 34\%\ H_2O_2) = 10/1$ (v/v) solution, *c* $[(n\text{-}C_4H_9)_4N]_2\{HPO_4[WO(O_2)_2]_2\}$ freshly prepared solution in $CH_3CN/(\sim 34\%\ H_2O_2) = 10/1$ (v/v); ~25 °C

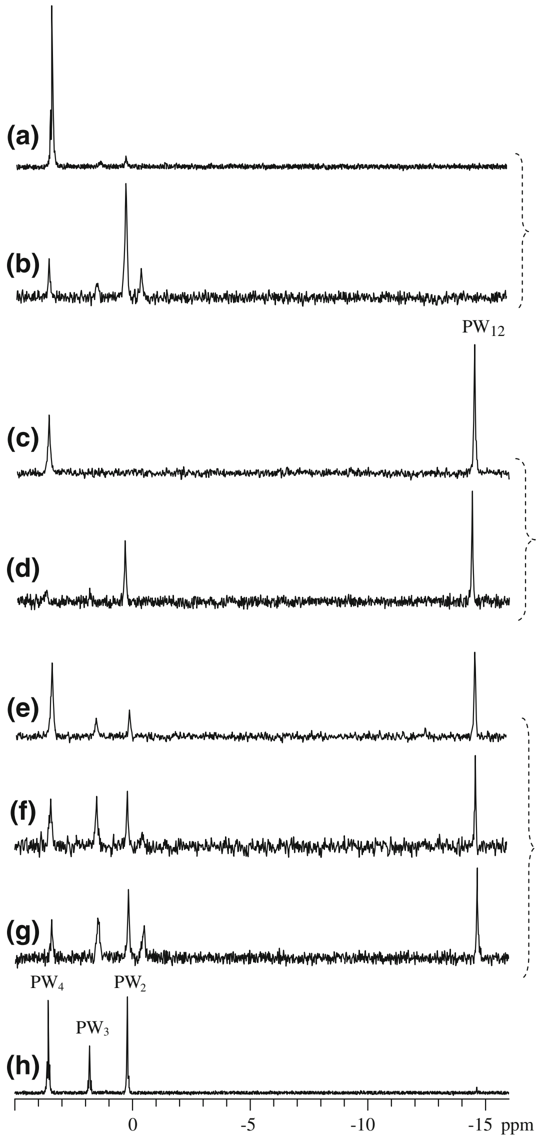

Fig. 3 ^{31}P NMR spectra of the reaction solutions *a*, *c*, *e* without BD and *b*, *d*, *f*, *g* in the process of the catalytic reaction with BD at catalysts and H_2O_2 concentrations as in Fig. 1. *a*, *b* TBA-PW_4, *c*, *d* TBA-PW_{11}, *e*–*g* EMIm-PW_{11}, *h* horizontally compressed spectrum from Fig. 2b of the solution containing three identified peroxo complexes, used for reference (2,3 mM, except for *a*, *h* 10 mM), H_2O_2 (1 M), $CH_3CN/(\sim 34\%\ H_2O_2) = 10/1$ (v/v), *b*, *d*, *f* after adding BD 2 h, *g* 3, 5 h; 25 °C (*a*, *h*), 50 °C (*b*–*g*)

Scheme 1 Transformations of TBA-PW_{11} in H_2O_2 solution (1), during initial (2) and nearly stationary (3) period of the BD epoxidation

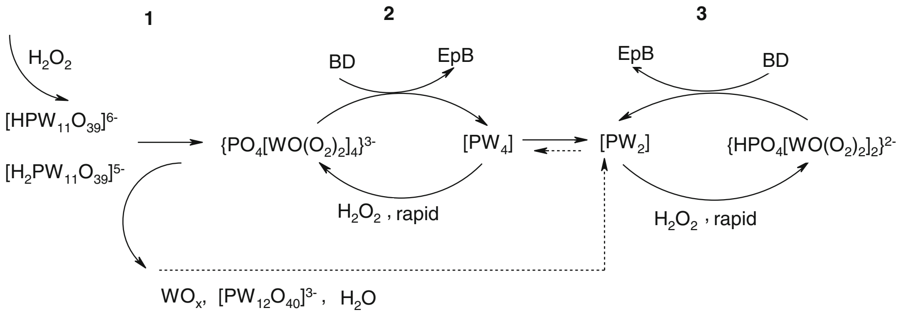

complexes $PW_3O_m^{\alpha-}$ (PW_3) (the satellites to central peak intensity ratio ~1:4.5:1) and $[HPO_4[WO(O_2)_2]_2^{2-}$ (PW_2) (~1:6:1) [23, 26, 27]. The assignment of the above peaks should not be based only on their chemical shift values that strongly depend on the solvent composition. Thus, $[(n\text{-}C_4H_9)_4N]_2\{HPO_4[WO(O_2)_2]_2\}$ in $MeCN/CDCl_3$ solution was observed at δ ~ 3 ppm [23], while we observed the same complex in CH_3CN solution at ~2 ppm. When CH_3CN contains 10% of water, the signal shifts to ~0.4 ppm (Fig. 2c). Another signal was detected at ~–0.3 ppm, when the spectra were recorded in the presence of both H_2O_2 and BD (Fig. 3b, g). It possibly arises from $PWO_n^{\beta-}$ (PW_1) peroxo complex, but it is too weak for observing its $^2J_{P\text{–}O\text{–}W}$ satellites (~1:12:1). Thus, we identified the three species observed in CH_3CN solutions of phosphotungstates after adding aqueous H_2O_2 in a large excess, as peroxo complexes PW_4, PW_3 and PW_2 The signals of the peroxo complexes are inversely ordered in these solutions (Fig. 2h) in comparison to their aqueous solutions [23]. Some other phosphotungstate peroxo complexes were observed only with lower hydrogen peroxide content [18, 22, 27].

The salt TBA-PW_{11} (of overall compozition $(TBA)_{5\text{-}}Na_{0,6}H_{1,4}[PW_{11}O_{39}]$) dissolved in CH_3CN (10 mM) gives two broad signals (−12.3 and −12.8 ppm) that coalesce into a single narrow peak (−12.5 ppm) when water is added ($CH_3CN/H_2O = 10/1$, v/v) (Fig. S1, b, c). The above two signals relate to polyanions $[HPW_{11}O_{39}]^{6-}$ and $[H_2PW_{11}O_{39}]^{5-}$, observed by an averaged signal due to fast proton exchange in the presence of water. The intensity ratio of the signals, equal to ~1.4:1, corresponds to an average degree of protonation of the polyanions in the TBA-PW_{11} salt, found by the chemical analysis. Protonated state of the polyanions is indicated by the high frequency shift of their signals as compared with aqueous solution of Na-PW_{11} (−10.7 ppm, pH 4.5–7.5) containing polyanions $[PW_{11}O_{39}Na]^{6-}$ [36]. Crystallization of mixed acidic salts, such as $Na_2[N(CH_3)_4]_4H[PW_{11}O_{39}]\bullet 7H_2O$ [43], is typical for bulky organic cations due to steric hindrance.

Dissolving TBA-PW_{11} in $CH_3CN/(\sim 34\%\ H_2O_2) = 10/1$, v/v under the reaction conditions, corresponding to 2.3 mM TBA-PW_{11} and ~1 M H_2O_2, 50 °C, resulted in full conversion of $[HPW_{11}O_{39}]^{6-}$ and $[H_2PW_{11}O_{39}]^{5-}$ anions to $\{PO_4[WO(O_2)_2]_4\}^{3-}$ and $[PW_{12}O_{40}]^{3-}$ (stage 1 in Scheme 1) in the ratio of ~40:60% (Fig. 3c). The process of the conversion was followed at ~20 °C (Fig. S1, d–f).

EMIm-PW_{11} salt is scarcely soluble in CH_3CN and in CH_3CN/H_2O, but under the reaction conditions it completely dissolved converting to $\{PO_4[WO(O_2)_2]_4\}^{3-}$ (~40%), $[PW_{12}O_{40}]^{3-}$ (35%), and new species observed by signals at ~2 and 0.4 ppm (25% in sum) (Fig. 3e). These two signals can be assigned to peroxo complexes PW_3 and PW_2 from comparing with the spectrum of a mixture of the reference compounds (Fig. 3h).

In the process of the catalytic reaction of BD with H_2O_2, the NMR measurements were made in the following way. One hour after starting catalysis, the reaction solution, 2.5 mL, with the same as in kinetic measurements (Fig. 1) concentrations of H_2O_2 (~1 M) and the catalyst (2.3 mM), was poured from the glass reactor into an NMR ampoule in the flow of BD. The ampoule was sealed hermetically and set into the spectrometer at 50 °C to maintain the near-reaction conditions. Spectra were measured periodically for several hours. Each spectrum was accumulated for 20–40 min. The spectra obtained are also shown in Fig. 3.

When we started from TBA-PW_4 and TBA-PW_{11}, peroxo complex PW_4 was stable in the presence of H_2O_2 before contacting with BD, but transformed almost completely to the other peroxo complexes in the process of the reaction with BD and H_2O_2, with PW_2 being predominant independently of the composition of starting complexes (Fig. 3b, d). In the case of EMIm-PW_{11}, the peroxo complexes appeared to be more stable. The spectrum only partly changed in the process of reaction with BD and H_2O_2, the PW_3 and PW_2 amounts increasing a little (Fig. 3f).

In addition to $\{PO_4[WO(O_2)_2]_4\}^{3-}$, other phosphotungstate peroxo complexes were regarded elsewhere as active intermediates in epoxidation of olefins [24, 29]. We related initial and stationary rates of EpB formation estimated from curves a–c in Fig. 1, to concentrations of the peroxo complexes, calculated from ^{31}P NMR spectra in Fig. 3, before and 2 h after adding BD (Table 3, entries 1–3 and 4–6, respectively).

$PW_{12}O_{40}{}^{3-}$ anion is not active in epoxidation because it does not contain peroxo groups. It persists in CH_3CN/($\sim$34% H_2O_2) = 10/1 solution (^{31}P NMP: the only peak at −14.6 ppm for $(TBA)_3PW_{12}O_{40}$ and $H_3PW_{12}O_{40}$).

In addition to phosphotungstate species, reaction solutions contain polyoxo tungstate, WO_x, released during rearrangements of the initial complexes. Its concentration was evaluated from the balance and is also given in Table 3. To elucidate possible contribution of polyoxo tungstate in the BD epoxidation, we prepared peroxotungstate anion $[W_2O_3(O_2)_4(H_2O)_2]^{2-}$ according to [44] in aqueous solutions of sodium tungstate and H_2O_2 by adding HCl until pH 3.8 and 2.25. We tested the obtained solutions in the catalytic reaction at CH_3CN 2 mL, $\sim$34% aq. H_2O_2 2 mmol, BD 1 mmol, 50 °C and W concentrations corresponding to those given in Table 3. The amount of EpB formed for 1 h of reaction did not exceed 7 mmol L^{-1}. It means that peroxotungstate, that could form under the reaction conditions, was significantly less effective in the BD epoxidation than the phosphotungstate peroxo complexes.

The initial period of the catalytic reaction was characterized by a maximum concentration of PW_4 and, correspondingly, by the highest rate of the EpB formation (stage 2 in Scheme 1). The initial rate of the EpB formation estimated from amount of EpB produced for the first hour of the reaction was nearly proportional to the concentration of PW_4 for TBA-PW_4 and TBA-PW_{11} (Table 3, entries 1, 2). The highest activity of the EMIm-PW_{11} corresponded to the largest total concentration of the peroxo complexes (Table 3, entry 3).

The EpB formation in a nearly stationary state characterized by linear parts of the kinetic curves (Fig. 1a–c) becomes slower. In this period (2–5 h), PW_x ($x < 4$) peroxo complexes appear (stage 3 in Scheme 1) which are suggested to be less active than PW_4. To verify this suggestion, we compared activities of TBA-PW_4 and purposely prepared TBA-PW_2 in oxidation of BD with H_2O_2 under conditions given in Table 2, entry 1. The TBA-PW_2 did show 3 times lower activity as compared with TBA-PW_4. In agreement with this observation, transformation of starting TBA-PW_4 into PW_2 resulted in about 3 time decrease in the rate as compared with the initial period of the reaction (Table 3, entries 1 and 4). Entries 5 and 6 show improving action of the $EMIm^+$ cation on stability of more active PW_4 and PW_3 peroxo complexes under the catalytic conditions. As a result, the stationary rate of the EpB formation was higher with EMIm-PW_{11} than TBA-PW_{11} catalyst.

However, correlation of the stationary rate with concentration of peroxo complexes is not regular, if we consider different phosphotungstates. Thus, the stationary rates of EpB formation were equal for the TBA-PW_4 and TBA-PW_{11} catalysts, although the concentration of the observed PW_2 peroxo complex was lower in the TBA-PW_{11} solution (Table 3, entries 4 and 5). The difference may be connected with the influence of some other tungsten species on the catalytic process. Apart from the possible minor contribution of peroxotungstate to the total catalytic activity, tungstate and also PW_{12} ions can promote regeneration of the more active PW_4 and PW_3 peroxo complexes under turnover conditions, thus increasing the stationary rate.

Depicted for TBA-PW_{11}, Scheme 1 shows transformations of catalyst during the BD epoxidation. During initial period, the BD epoxidation proceeds through its interaction with $\{PO_4[WO(O_2)_2]_4\}^{3-}$ complex to form [PW_4], so called, “subsequent peroxo species” [27]. The complex is rapidly regenerated with H_2O_2, at the same time, being able to depolymerize to form the other active peroxo complexes ($\{HPO_4[WO(O_2)_2]_2\}^{2-}$ in Scheme 1). Suggested reverse process is shown with dashed arrows. Full regeneration of Keggin type phosphotungstate catalysts after complete hydrogen peroxide consumption was earlier shown in the related systems [19, 29].

4 Conclusions

Phosphotungstates catalyze epoxidation of 1,3-butadiene with aqueous H_2O_2 in acetonitrile solution. High selectivity of the BD and H_2O_2 to EpB conversion was kept in a wide range of temperature and the peroxide concentration. Competitive radical reactions of the BD oxidation and H_2O_2 decomposition were minimized. The catalytic activity of the phosphotungstates depends on the composition of the both anionic and cationic moieties and changes in the row: $(TBA)_3\{PO_4[WO(O_2)_2]_4\} \approx (TBA)_5Na_{0.6}H_{1.4}[PW_{11}O_{39}] < (EMIm)_5NaH[PW_{11}O_{39}]$.

The composition of the reaction solutions in the presence of H_2O_2 and in the process of the catalytic reaction of H_2O_2 with BD was established by the ^{31}P NMR spectroscopy, and related to the starting and stationary rates of oxidation of BD. The $\{PO_4[WO(O_2)_2]_4\}^{3-}$ peroxo complex, predominating in H_2O_2 solutions of phosphotungstates, provide maximal activity of the systems during the initial period of the catalytic reaction. At the nearly stationary period, this complex partially or completely transforms to less active peroxo complexes $PW_nO_m^{\alpha-}$, $n = 3, 2, 1$. The enhanced efficiency of $(EMIm)_5NaH[PW_{11}O_{39}]$ in comparison to $(TBA)_5Na_{0,6}H_{1,4}[PW_{11}O_{39}]$ can be explained by higher concentration of the active peroxo complexes in the reaction solution.

References

1. Cheeseman N, Fox M, Jakson M, Lennon IC, Meek G (2004) Proc Nat Acad Sci USA 101:5396
2. Remains TJ, van Oeffelen D, Steijns M, Martens JA, Jacobs PA (1998) J Catal 175:312

3. Musolino MG, Apa G, Donato A, Pietropaolo R (2005) Catal Today 100:467
4. Matsuno H, Odaka K (1997) JP 09110850
5. Monnier JR, Muchlbauer PJ (1990) US Patent 4.897.498
6. Monnier JR (2001) Appl Catal 221:73
7. Zhang X, Zhang Z, Suo J, Li S (2000) Catal Lett 66:175
8. Liu Y, Murata K, Inaba M, Mimura N (2005) Appl Catal B 58:51
9. Blanko-Brieva G, Capel-Sanchez MC, Pilar de Frutos M, Padilla-Polo A, Campos-Martin JM, Fierro JLG (2008) Ind Eng Chem Res 47:8011
10. Mizuno N, Yamaguchi K, Kamata K (2005) Coord Chem Rev 249:1944
11. Kamata K, Katani M, Yamaguchi K, Hikichi H, Mizuno N (2007) Chem Eur J 13:639
12. Mirkhani V, Moghadam M, Tangestaninejad S, Mohammodpoor-Baltork I, Shams E, Rosouli N (2008) Appl Catal A 334:106
13. Liu L, Chen C, Hu X, Mohamood T, Ma W, Lin J, Zhao J (2008) New J Chem 32:283
14. Zhao W, Ma B, Hua H, Zhang Y, Ding Y (2008) Catal Commun 9:2455
15. Zhao W, Ding Y, Zhang Z, Ma B, Qiu W (2011) Reac Kinet Mech Cat 102:93
16. Capel-Sanchez MC, Campos-Martin JM, Fierro JLG (2010) Catal Today 158:103
17. Liu X, Jeffries HE, Sexton KG (1999) Atmos Environ 33:3005
18. Kuznetsova LI, Maksimovskaya RI, Fedotov MA, Matveev KI (1983) Izv Akad Nauk SSSR ser khim (Engl Transl) 666
19. Kuznetsova LI, Maksimovskaya RI, Fedotov MA (1985) Izv Akad Nauk SSSR ser khim (Engl Transl) 488
20. Venturello C, D'Aloisio R, Bart JCJ, Ricci M (1985) J Mol Cat 32:107
21. Ishii Y, Jamawaki K, Yoshida T, Ura T, Ogawa M (1987) J Org Chem 52:1868
22. Aubry C, Chottard G, Platzer N, Brégeault J-M, Thouvenot R, Chauveau F, Huet C, Ledon H (1991) Inorg Chem 30:4409
23. Salles L, Aubry C, Thouvenot R, Robert F, Dorémieux-Morin C, Chottard G, Ledon H, Jeannin Y, Brégeault J-M (1994) Inorg Chem 33:871
24. Mahha Y, Salles L, Piquemal J-Y, Briot E, Atlamsani A, Brégeault J-M (2007) J Catal 249:338
25. Kuznetsova NI, Detusheva LG, Kuznetsova LI, Fedotov MA, Likholobov VA (1992) Kinet. Katal 33:516 [Kinet Catal 33: 415 (Engl Transl)]
26. Dengel AC, Griffith WP, Parkin BC (1993) J Chem Soc Dalton Trans 2683
27. Duncan DC, Chambers RC, Hecht E, Hill CL (1995) J Am Chem Soc 117:68
28. Gresley NM, Griffith WP, Laemmel AC, Nogueira HIS, Parkin BC (1997) J Mol Catal Chem 117:185
29. Gao J, Chen Y, Han B, Feng Z, Li C, Zhou N, Gao S, Xi Z (2004) J Mol Catal Chem 210:197
30. Valente AA, Petrovski Z, Branko LC, Alfonso CAM, Pillinger M, Lopes AD, Romão CC, Nunes CD, Goncalves IS (2004) J Mol Catal Chem 218:5
31. Chhikara BS, Chandra R, Tandon V (2005) J Catal 230:436
32. Bortolini O, Conte V, Chiappe C, Fantin G, Fogagnolo M, Maietti S (2002) Green Chem 4:94
33. Berardi S, Bonchio M, Carraro M, Conte V, Sartorel A, Scorrano G (2007) J Org Chem 72:8954
34. Wang S-S, Liu W, Wan Q-X, Liu T (2009) Green Chem 11:1589
35. Kumar A (2007) Catal Commun 8:913
36. Maksimovskaya RI (1998) Russ J Inorg Chem 43:1822
37. Cammarata L, Kazarian SG, Salter PA, Welton T (2001) Phys Chem Chem Phys 3:5192
38. Lin S-T, Ding M-F, Chang C-W, Lue S-S (2004) Tetrahedron 60:9441
39. Maksimov GM, Kustova GN, Matveev KI, Lazarenko TP (1989) Koord Khim 15:788
40. Hendry DG, Mayo FR, Schuetzle D (1968) Ind Eng Chem Prod Res Dev 7:136
41. Kozlov YN, Nizova GV, Shul'pin GB (2004) Zhurn Fiz Khim 78:248
42. Kozlov YN, Nizova GV, Shul'pin GB (2005) J Mol Catal Chem 227:247
43. Fuchs J, Thiele A, Palm R (1981) Z Naturforsch 36B:544
44. Campbell NJ, Dengel AC, Edvards CJ, Griffith WP (1989) J Chem Soc Dalton Trans 1203